Brain Struct Funct (2013) 218:59–72
DOI 10.1007/s00429-011-0376-z

ORIGINAL ARTICLE

Hippocampal microRNA-132 mediates stress-inducible cognitive deficits through its acetylcholinesterase target

G. Shaltiel · M. Hanan · Y. Wolf · S. Barbash · E. Kovalev · S. Shoham · H. Soreq

Received: 7 November 2011 / Accepted: 29 December 2011 / Published online: 14 January 2012

Abstract Diverse stress stimuli induce long-lasting cognitive deficits, but the underlying molecular mechanisms are still incompletely understood. Here, we report three different stress models demonstrating that stress-inducible increases in microRNA-132 (miR-132) and consequent decreases in its acetylcholinesterase (AChE) target are causally involved. In a mild model of predator scent-induced anxiety, we demonstrate long-lasting hippocampal elevation of miR-132, accompanied by and associated with reduced AChE activity. Using lentiviral-mediated suppression of "synaptic" AChE-S mRNA, we quantified footshock stress-inducible changes in miR-132 and AChE and its corresponding cognitive damages. Stressed mice showed long-lasting impairments in the Morris water maze. In contrast, pre-stress injected AChE-suppressing lentivirus, but not a control virus, reduced hippocampal levels of both miR-132 and AChE and maintained similar cognitive performance to that of naïve, non-stressed mice. To dissociate between miR-132 and synaptic AChE-S as potential causes for stress-inducible cognitive deficits, we further used engineered TgR mice with enforced over-expression of the soluble "readthrough" AChE-R variant without the 3′-untranslated region binding site for miR-132. TgR mice displayed excess AChE-R in hippocampal neurons, enhanced c-fos labeling and correspondingly intensified reaction to the cholinergic agonist pilocarpine. They further showed excessive hippocampal expression of miR-132, accompanied by reduced host AChE-S mRNA and the GTPase activator p250GAP target of miR-132. At the behavioral level, TgR mice showed abnormal nocturnal locomotion patterns and serial maze mal-performance in spite of their reduced AChE-S levels. Our findings attribute stress-inducible cognitive impairments to cholinergic-mediated induction of miR-132 and consequently suppressed ACHE-S, opening venues for intercepting these miR-132-mediated damages.

Keywords Acetylcholinesterase · P250GAP · Cholinergic · Cognition · MicroRNA-132 · Psychological stress

Shaltiel G and Hanan M contributed equally.

Electronic supplementary material The online version of this article (doi:10.1007/s00429-011-0376-z) contains supplementary material, which is available to authorized users.

G. Shaltiel · M. Hanan · Y. Wolf · S. Barbash · H. Soreq (✉)
The Edmond and Lily Safra Center of Brain Sciences,
The Silberman Institute of Life Sciences,
The Hebrew University of Jerusalem,
Jerusalem 91904, Israel
e-mail: soreq@cc.huji.ac.il

E. Kovalev · S. Shoham
Herzog Memorial Hospital, Jerusalem 91351, Israel

Introduction

Acute and chronic stress can both induce anxiety (McEwen and Gianaros 2011) and either impair learning and memory performance (Diamond et al. 1999; Nijholt et al. 2004) or enhance it (Blank et al. 2002). Manipulating cholinergic neurotransmission in the hippocampus, which receives extensive cholinergic innervations, changes the cognitive control over executive function and error monitoring (Carter et al. 1998), suggesting cholinergic involvement in stress responses. Recent studies associate acute and chronic stress reactions with specific microRNA (miR)-mediated silencing of affected transcripts (Meerson et al. 2010). MiRs are short (~22 nucleotides), non-coding RNAs that

regulate various molecular pathways (Bartel 2009; Krol et al. 2010) by post-transcriptional gene silencing (Filipowicz et al. 2008; Rana 2007). Each miR may target several mRNAs, often in specific locations on their 3′-untranslated region (3′-UTR) and can modulate entire pathways in a rheostat-like manner (Chen et al. 2004) [reviewed in (Soreq and Wolf 2011)]. However, the signaling pathway(s) controlling the levels of neuronal miRs, the corresponding miR-target interactions involved in their diverse functions and the consequent cognitive effects remain incompletely understood.

MiR-132 is prominently neuronal-enriched, highly induced by the cAMP-response element binding protein (CREB). In cortical neurons, miR-132 enhances neuronal morphogenesis and neurite outgrowth by decreasing the levels of the Rho family member GTPase-activating protein, p250GAP (Vo et al. 2005). Mice engineered to overexpress miR-132 in forebrain neurons correspondingly show marked increase in dendrite spine density, accompanied by deficits in a novel object recognition test (Wayman et al. 2008). However, which neurotransmission signal(s) are responsible for miR-132 changes and which of its target(s) mediate these effects remained unanswered.

Another target of miR-132 is the acetylcholine hydrolyzing enzyme acetylcholinesterase (AChE) (Shaked et al. 2009; Meshorer and Soreq 2006). In acute psychological stress, activated cholinergic neurons display rapid, yet transient increases in a normally rare soluble AChE-R splice variant (Kaufer et al. 1998) that replaces the "synaptic" AChE variant (Kaufer et al. 1998; Meshorer et al. 2002; Meshorer and Soreq 2006). In macrophages, AChE suppression by miR-132 accentuates cholinergic signaling (Shaked et al. 2009). In transfected neurons, tetracycline-controlled antisense suppression of AChE leads to enhanced dendrite extension and causes hyper-locomotion in engineered mice (Sklan et al. 2006). Taken together, we surmised that miR-132-mediated suppression of hippocampal AChE levels may enhance cholinergic signaling, contributing to the neurite extension, cognitive and locomotion impairments caused by stressful experiences.

To challenge these predictions, we sought appropriate mouse models and experimental strategies. Our rationale was as follows: (1) If indeed stress-inducible changes in hippocampal miR-132 and AChE cause long-lasting effects, miR-132 increases and AChE activity decreases should be observed in different stress models and even several days after the initiation of psychological stress. (2) If the changes in miR-132 and "synaptic" AChE-S are inter-related, then preventing one would avoid the other, and if these changes are the cause for stress-induced cognitive deficits, then preventing them both from happening would avoid these deficits. (3) Alternatively, if miR-132 elevation by itself is sufficient to cause the stress phenotype and cognitive malfunctioning, then maintaining miR-132 excess even under AChE-S suppression would cause cognitive deficits.

To investigate this triple hypothesis, we employed three diverse stress paradigms: the acute predator scent test, acute unpredictable footshocks accompanied by hippocampal AChE knockdown, and engineered mice with an inherited anxiogenic-like phenotype (Salas et al. 2008) due to enforced excess of AChE-R, but with a depleted miR-132 binding site which ensures continuous suppression of the host AChE-S, but not the transgenic AChE-R proteins (Shaked et al. 2009). In the two latter models, we also evaluated cognitive deficits evolving from the stress exposure.

Methods

Animals

Mice were kept in an animal room at a constant temperature (22 ± 1°C) and a 12-h light/dark cycle with free access to food and water. They were tested in the same room under dim illumination (30 lux) by the same testers between 10 and 16 h. All experimental procedures were approved by The Hebrew University's Committee for Animal Experimentation (NS-08-11485-4).

Pharmacological intervention

Intraperitoneal (i.p) injection of 0.1 ml of 25 mg/kg pilocarpine hydrochloride (Sigma, Rehovot, Israel), or saline followed 30 min habituation to a holding cage.

Stereotactic surgeries

Group housed C57Bl/6J 9 weeks old male mice underwent stereotactic surgery, after which they were singly-housed throughout all subsequent testing. Control mice were singly housed as well. Mice were anesthetized by i.p. injections of ketamine (50 mg/kg) (Forth Dodge, IA, USA) and domitor (0.5 mg/kg) (Orion Pharma, Espoo, Finland) mix, and then mounted in a stereotactic apparatus for intra-hippocampal injections. Coordinates of the injection sites (in mm) relative to bregma were AP: −2.0, L: 1.8, DV: −1.5. Bilateral injections of 0.5 ul lentiviral suspensions were conducted using a 10-l Glenco syringe (Houston, TX, USA). After each injection, the needle was left in situ for 5 min before being retracted to allow complete diffusion.

Water maze test

The water maze consisted of a round tank, 1.6 m in diameter, filled with water. Mice were trained to find the

location of a hidden platform (16 cm in diameter), submerged 1 cm below the water surface, using extra maze visual cues. The training part consisted of 4 trials per day, with a 1-h brake between trials, for 3 days. The escape latency, i.e., the time required by the mouse to find the platform and climb on it, was recorded for up to 60 s. Each mouse was allowed to remain on the platform for 30 s and was then moved from the maze to its home cage. If the mouse did not find the platform within 60 s, it was placed gently on the platform for 30 s, and then returned to its home cage. On the fourth day of the experiment, the platform was removed and a probe trial was conducted: mice were placed in the maze for 60 s, in which the number of crosses over the four quadrants of the maze was recorded. Increased swimming in the quadrant where the platform was originally placed was considered as an indication of spatial acquisition. One day after the end of behavioral tests mice were anesthetized by Isoflurane inhalation and decapitated. Brains were removed and two half sagital sections were immediately frozen in liquid nitrogen. One section was sliced in cryostat for Karnovsky–Roots staining experiments (Sternfeld et al. 2000) and the other was taken for mRNA measurements. In brief, AChE activity staining was conducted using the Karnovsky–Roots staining method (Karnovsky and Roots 1964; Kaufer et al. 1998). 40-um frozen sections were incubated at room temperature in soft shaking for 5 min. Staining solution contained 2 mM acetylthiocholine iodide (Sigma, Israel), dissolved in PBS, 5 mM sodium citrate, 3 mM cupric sulfate, 0.5 mM potassium ferricyanide, 0.1 mM butyrylcholinesterase specific inhibitor, ISO-OMPA.

Two unit serial maze

3- to 6-months-old female 3′ UTR-null AChE and FVB/N mice were group housed. Only females were taken for this experiment due to their higher stress responsiveness compared with males (Goel and Bale 2010). Modular units placed in a series constitute this maze (Quartermain et al. 1994). To complete one "run", a 22 h water-deprived mouse must choose between turning right or left to receive, at the end of the maze, a reward in the form of 40 μl of 5% sucrose and one "run" is considered complete. Then the mouse must shuttle back to the other end of the maze where it gets the same reward. There were 5 runs per session; one session per day. Quantitative measures of performance include number of left/right choice errors and "retrace errors"—episodes in which a mouse moves in the wrong direction (toward the end without a reward) (Farchi et al. 2007). Mice were euthanized 80–90 min after the behavioral experiment by an intra-peritoneal injection of 200 mg/kg sodium pentobarbital ("Pental"). Brains were either fixed by transcardial perfusion with ice-cold 4% paraformaldehyde containing 4% sucrose (pH 7.4) or removed and kept frozen in −70°C.

Predator scent exposure and footshock acute stress

Group housed C57Bl/6J 9 weeks old male mice were placed on well-soiled cat litter for 10 min (in use by the cat for 2 days, sifted for stools) (Cohen et al. 2006) or were placed in a footshock delivery system (Campden Instruments, UK) where they received seven inescapable electric footshocks (0.3 mA; 2 ms) at unequal intervals over a total period of 120 min.

Elevated plus maze

Anxiety-related behaviors were tested in a Plexiglas plus-shaped maze containing two dark and enclosed arms (30 × 5 cm with a 5 × 5 cm center area and 40 cm high walls) and two 30 × 5 cm open and lit arms, all elevated 50 cm above ground. Individual mice were placed in the center of the maze, tracked for 5 min with a video camera, and then returned to their home cage. The plus maze was wiped clean between trials with a 10% alcohol solution.

Lentiviral procedures

The packaged virus was collected at 24 and 48 h post-transfection and concentrated using ultracentrifugation (70,000*g*, 2 h, 15°C). Dilutions of concentrated virus were followed by infection of HEK-293T cells with diluted virus. The resulting titer ($\sim 1 \times 10^9$ infectious particles per ml) was assessed for shRNA expressing viruses using puromycin selection and for GFP expressing viruses by cell fluorescence counting. Screening of two putative AChE shRNAs, sh799 and sh800, designed to down-regulate mouse/rat AChE levels was first conducted in neuronal-like PC12 cells and compared to a control shRNA (shCON) that does not target any mammalian gene. Both shRNAs reduced the AChE-S variant and suppressed AChE total activity in these cells, but only Sh799 down-regulated overall AChE mRNA levels (Online Resources Fig. 1).

Viral infection of primary cortical cell culture

Cerebral cortex was separated from the brain of 15th day embryos of FVB/N mice, minced, and cells plated on poly-L-ornithine coated 12-well plates in Neurobasal medium, 2% B27 supplement, 20% Glutamax and 20% Penicillin/streptomycin (Invitrogen, Grand Island, NY, USA). 72 h post-plating, 250 ul of non-concentrated medium containing viral particles was added to each well.

RNA procedures

RNA was extracted (RNeasy lipid tissue kit, Qiagen, Valencia, CA, USA), DNase treated and its integrity confirmed by gel electrophoresis.

For SYBR green real-time PCR, cDNA synthesis (Promega, Madison, WI, USA) involved 1 μg RNA samples in 20 μl reactions. Duplicate real-time reverse transcriptase (RT) PCR tests involved ABI prism 7900HT, SYBR green master mix (Applied biosystems, Foster City, CA, USA) and ROX, and a passive reference dye for signal normalization across the plate. Primer sequences are listed in Table 1. 18S rRNA or GAPDH was used as reference transcripts. Annealing temperature was 60°C for all primers. Serial dilution of samples served to evaluate primers efficiency and the appropriate cDNA concentration that yields linear changes. Melting curve analysis and amplicons sequencing verified the identity of end products.

MicroRNA quantification using The TaqMan MicroRNA Assays (Applied Biosystems, Foster City, CA, USA) was conducted in two-step RT-PCR kit according to the manufacturer's instructions. For miR-132 (Applied Biosystems, Foster City, CA, USA) measurements, a reference transcript of SNO-135 (Applied Biosystems) was used.

Histochemistry and immunohistochemistry

The AChE-R C-terminal peptide (ARP) was labeled by a rabbit polyclonal antibody (Berson et al. 2008). The common domain shared by both AChE variants was labeled with goat anti-human AChE (Santa Cruz, CA, USA, antibody N19). c-fos was stained using rabbit anti c-fos (Sigma, Rehovot, Israel). In co-localization studies, we used fluorescein (FITC)-labeled donkey anti-rabbit to visualize AChE-R and streptavidin-Cy3 to visualize general AChE. Two to three coronal brain sections were sampled at an estimated distance of 2.8–3.3 mm posterior to bregma. Images of each hippocampal sub-region were acquired and analyzed using AnalySIS software (SIS, Germany). Karnovsky staining of histochemical AChE activity was as in (Sternfeld et al. 2000). In situ hybridization was essential as described (Berson et al. 2008).

AChE activity measurement

AChE activity was measured by Ellman's assay (Ellman et al. 1961) adjusted to multiwell plates and normalized according to the protein content of the cell lysate (DC™ protein assay, Bio-Rad, Hercules, CA, USA).

Statistical analysis

The following statistical analyses were done using STATISTICA9 and GraphPad Prism 5 software: Student's *t* test, one-way ANOVA and two-way ANOVA with Tukey post hoc comparisons and Pearson's correlation test.

Results

Elevated predator stress-inducible miR-132 associates with suppression of AChE-S

Our first experimental model served to explore the interrelationship between a long-lasting stress phenotype, induced by predator scent, increases in hippocampal miR-132 and decreases in AChE-S. Seven days following a predator scent stress (Fig. 1a), C57BI/6J mice subjected to an elevated plus maze (EPM) showed sustained anxiety. Compatible with previous reports on predator smell-stressed mice (Cohen et al. 2006), they spent less time in the maze open arms and more time in its closed arms and attempted fewer entries to the open arms compared to naïve mice (Fig. 1b–d). Given that miR-132 targets the AChE

Table 1 Primer sequences for SYBR green real-time PCR

Isoform	Forward primer 5′–3′	Reverse primer 5′–3′
mAChE common	cggaggctctcatcaatac	accccgtaaaccagaaagtag
mAChE-S	ctgaacctgaagcccttagag	ccgcctcgtccagagtat
mAChE-R	gagcagggaatgcacaag	ggggaggtaaagaagagag
hAChE-R	cttcctccccaaattgctc	ggggagaagagaggggttac
mP250GAP	accaactcagtgccaaaacc	aacccagaattgaggaggtg
m18S rRNA	cgccgctagaggtgaaattc	ttggcaaatgctttcgcgcgtc
mGAPDH	atcaagaagtggtgaagcag	cctactccttggaggccatgt
rAChE common	cggacgctctcatcaatac	acccccgtaaaccagaaagtag
rAChE-S	ctgaacctgaagcctttggag	gcgctccgcctcgtccag
rAChE-R	gaacctgaagcctttgg	ccttttctctctcccgtcct
r18S rRNA	cgccgctagaggtgaaattc	ttggcaaatgctttcgcgcgtc

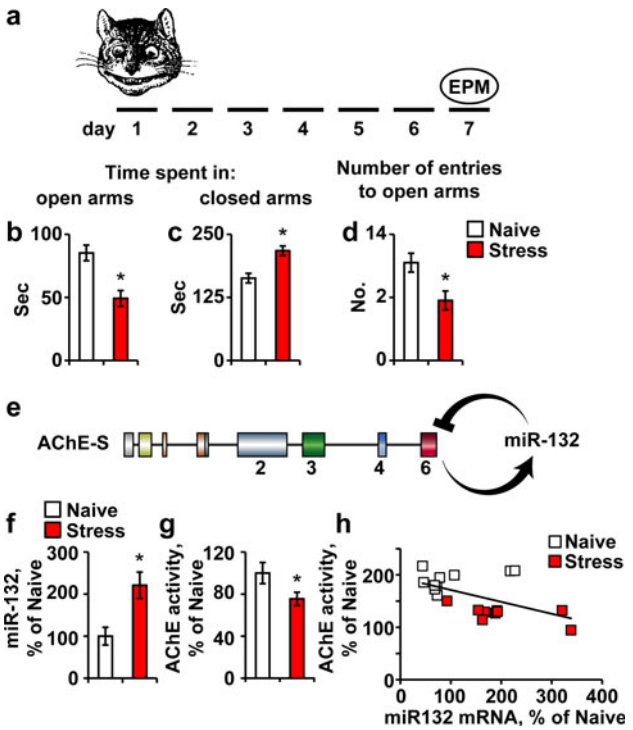

Fig. 1 Predator scent stress leads to inter-related miR-132 elevation and AChE and p250GAP suppression. **a** Mice were exposed to the predator scent test and 7 days later were tested in the elevated plus maze (EPM). **b–d** Compared to naïve, stressed mice spent less time in the open EPM arms (**b**; Student's t test: $^*p < 0.05$), more time in the closed EPM arms (**c**; $^*p < 0.05$) and attempted less entries to the open arms (**d**; $^*p < 0.05$). **e** AChE-S activation leads to miR-132 up-regulation, which in return down-regulates the AChE-S transcript. **f–h** 7 days post predator scent exposure, hippocampal miR-132 is up-regulated by ~220% (**f**; Student's t test, $t_{18} = -3.22$, $^*p < 0.01$), AChE activity is reduced (**g**; Student's t test, $t_{23} = 2.00$, $^*p < 0.05$) and hippocampal miR-132 levels show significant negative correlation to AChE activity (**h**; Pearson's test: $r = -0.55$; $p < 0.01$)

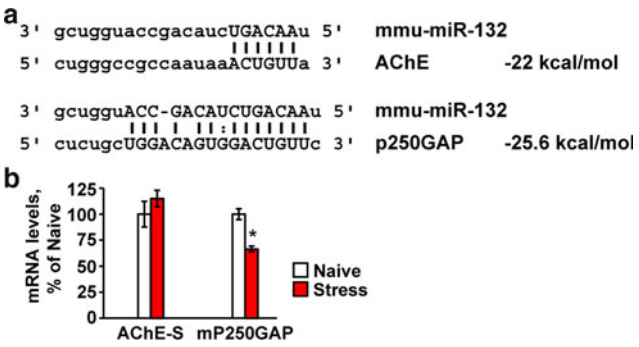

Fig. 2 Neuronal AChE and the GTPase activator p250GAP are both targets of miR-132. **a** The 'seed' region in miR-132 is complementary to the targeted 3′-UTR in the AChE-S and P250GAP transcripts [created using Targetscan and Pictar websites (Online Resources Table 1)]. **b** Hippocampal mP250GAP mRNA, but not mAChE-S levels are reduced in stressed compared to naïve mice (Student's t tests: $^*p < 0.05$), likely reflecting different balances between the rates of transcription and miR-132-mediated destruction of these two transcripts

mRNA transcript (Fig. 1e), we quantified hippocampal miR-132 levels, which we found to be higher by ~220% compared to naïve mice (Student's t test: $p < 0.01$; Fig. 1f), accompanied by 25% reduction in AChE activity (t test: $p < 0.05$; Fig. 1g). A significant negative correlation between hippocampal miR-132 levels and AChE activity suggested causal relationship (Pearson's test: $r = -0.55$; $p < 0.01$; Fig. 1h), compatible with the capacity of miR-132 to suppress AChE activity in cultured primary neurons (Online Resources Fig. 2).

Our previous findings showed stress-inducible increases in neuronal AChE gene expression (Meshorer et al. 2002; Meshorer and Soreq 2002). Given that mRNA levels reflect a steady state between its synthesis and degradation, we predicted that the observed decline in AChE activity could potentially mask a balance between increases in the "synaptic" AChE-S mRNA and miR-132-induced decreases in its levels. To find more information on miR-132 relationships with its neuronal targets, we quantified the major AChE-S mRNA and the p250GAP transcript, with predictably tighter hybridization and higher energy interaction with miR-132 (Fig. 2a). Intriguingly, p250GAP but not AChE mRNA levels were suppressed in the predator scent-stressed hippocampus (Student's t test: $p < 0.05$, Fig. 2b), suggesting less robust stress-inducible transcription and/or more efficient destruction of p250GAP mRNA under stress.

AChE-S knockdown prevents miR-132 up-regulation and memory impairments

Predicting that the stress-inducible changes in hippocampal miR-132/AChE-S impair the cholinoceptive capacities of hippocampal neurons (Gray et al. 1996), we next set out to establish an in vivo experimental model where these changes could be avoided. To achieve this goal, we introduced AChE knockdown. For this purpose, we used a pre-calibrated shACHE agent targeted to the exon2 common to the AChE-S and AChE-R transcripts (Fig. 3a) and which efficiently infected cultured primary neurons (Fig. 3b), reduced AChE activity by over 50% within 12–24 h post-infection (Fig. 3c) and suppressed AChE-S and AChE-R mRNA levels as well as the common domain shared by these two transcripts (Fig. 3d). Bilateral injection of this agent to the hippocampus CA1 region of this AChE-targeted lentiviral shRNA (shAChE) was then followed by a 10-days healing period. At this time point, long after the transient stress-inducible increases in hippocampal AChE have ceased, histochemical staining showed reduced AChE activity in the hippocampus of lentiviral injected mice, with predictably larger reduction of AChE activity in

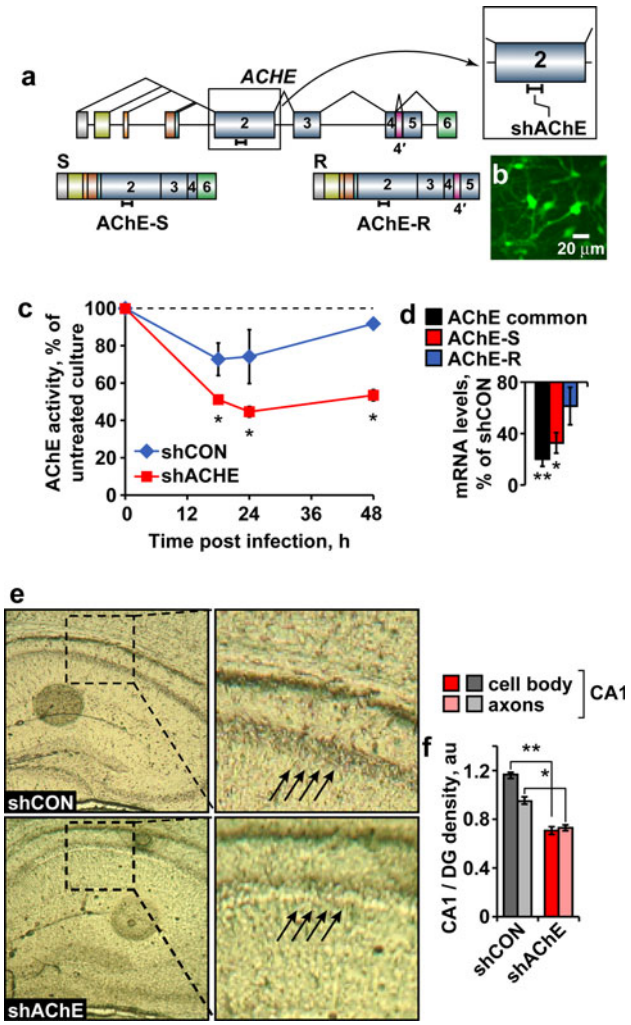

Fig. 3 Lentiviral mediated AChE-suppression in hippocampal neurons in vitro and in vivo. **a** The sh-799 agent is complementary to exon 2 in the endogenous mouse gene that is included in the two alternative transcripts. **b** Transduction efficiency of our GFP coding vector. Mouse primary cortical culture were transduced with vector coding for GFP (MOI = 1). Expression reveals high transduction efficiency, with more than 90% of cells being transduced. **c** Primary neuronal culture total AChE activity is suppressed 18, 24 and 48 h following viral infection with shAChE-S versus shCON. Two-way ANOVA: treatment ($F_{1,10} = 18.97$, $^*p < 0.01$), time ($F_{2,10} = 1.39$, p = NS) and interaction ($F_{2,10} = 0.46$, p = NS). **d** AChE splice variants mRNA levels in mouse cortical primary culture following treatment with sh799 versus shCON: overall AChE transcript was downregulated by 80% [$n = 4$ (sh799 and shCON); $^{**}p < 0.02$]. AChE-S was down-regulated by 68% [$n = 3$ (sh799 and shCON); Mann–Whitney U test: $^*p < 0.03$], while the considerably lower AChE-R mRNA levels remained unchanged [$n = 4$ (sh799), $n = 3$ (shCON); p = NS]. **e** Histochemical staining of AChE activity in shAChE or shCON treated hippocampal sections. **f** Reduced AChE activity in the shAChE versus shCON CA1 neuronal cell bodies and axons (relative to dentate gyrus; Student's t test; $t_{13} = 18.5$, $^{**}p < 0.001$ and $t_{13} = 5.24$, $^*p < 0.002$, respectively)

neuronal cell bodies compared to axons in the injected area (t test: $p < 0.001$ and $p < 0.002$, respectively; Fig. 3e, f) compared to hippocampi injected with a control virus.

AChE suppression prevents stress-inducible cognitive damages

Lentivirus-injected mice were subjected, 10 days post-injection, to unpredictable footshock stress compared to mice injected with a control virus (shCON) (Fig. 4a). Naïve and non-injected mice exposed to the footshock stress were tested in comparison. Similar to predator scent, footshock stress alone led to 63% increase in hippocampal miR-132, and infection with control lentiviruses extended the effect to a twofold increase in miR-132 levels. The effects on miR-132 of both stress and the chronic state of infection were completely prevented following shAChE suppression (one-way ANOVA: $p < 0.003$; Fig. 4b), suggesting that miR-132 elevation under stress is induced by the reduced cholinergic neurotransmission which is prevented by AChE suppression. In rotorod tests, injected mice showed normal performance reflecting unimpaired motor coordination (Online Resources. Fig. 3). Nevertheless, all of the stressed mice, regardless of their treatment spent less time in the open arms of the maze compared to naïve mice (one-way ANOVA: $p < 0.001$; Fig. 4c), demonstrating that preventing miR-132 increases failed to avoid the stress-inducible anxiety.

In the Morris water maze test, both shAChE-injected stressed mice and naïve mice learned to reach the hidden platform faster than either non-injected or shCON-injected stressed mice (post hoc test: $p < 0.05$ for both, Fig. 4d), which exhibited spatial learning deficits. By the third day of learning trials, all four groups displayed the same escape latencies; however, in the probe test, shAChE-injected mice showed control-like spatial memory, unlike the deficits shown by the stressed non-injected and shCON-injected groups. Both naïve and shAChE-injected stressed mice crossed more frequently over the missing platform quadrant, deviating from either non-injected or shCON-injected mice, at least in one time point; demonstrating better learning capacity to reach the hidden platform and reflecting better spatial memory (two-way ANOVA: $p < 0.05$; Fig. 4e, f).

shAChE-treated mice showed better cognitive performance that could potentially be due to the enforced decreases in AChE-S, the prevented increases in miR-132, corresponding changes in other transcripts (e.g., p250GAP) or to all of these reasons combined. To test for probable correlations between the measured molecular elements and the modified cognitive performance of stressed mice, we plotted the route traversed by each mouse in the first quadrant as a function of the levels of relevant RNA transcripts. Impressively, miR-132 levels in both control and shRNA-injected mice showed a significant correlation to the cognitive malfunction reflected in the route traversed in the missing platform quadrant during the probe test

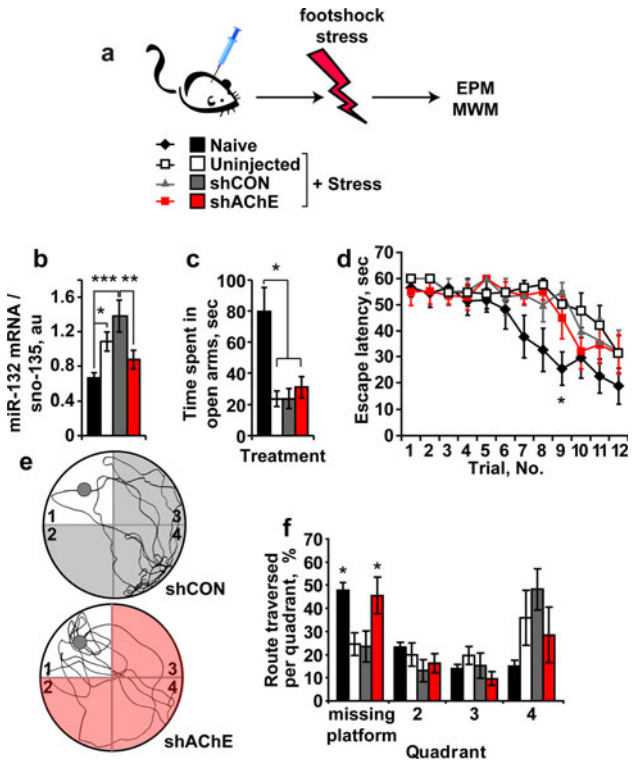

Fig. 4 AChE knockdown prevents the cognitive decline following footshock stress. **a** Mice subjected to CA1 hippocampal injection of lentivirus-mediated knockdown of AChE (shAChE) or irrelevant control virus (shCON) and un-injected stressed and naïve mice were exposed 3 weeks later to 7 unpredicted and inescapable footshock stress followed by EPM and Morris water maze (MWM) tests. **b** Hippocampal miR-132 mRNA levels increase by 63 and 100% in stressed and shCON stressed mice, but remained unchanged in shAChE stressed mice. ANOVA test: $F_{3,28} = 6.14$, $p < 0.003$. Post hoc LSD test: naïve versus stressed $*p < 0.05$, versus shCON-infected and stressed $***p < 0.001$; shCON-infected and stressed versus shAChE-infected and stressed mice $**p < 0.01$. **c** Naïve mice spend more time in the EPM open arms than all stressed groups (one-way ANOVA: $F_{3,28} = 8.49$, $p < 0.001$). **d** Naïve and shAChE-infected stressed mice learn to reach the MWM hidden platform faster than stressed or shCON stressed mice. Two-way ANOVA: trial number ($F_{11,323} = 12.33$, $p < 0.001$), treatment ($F_{3,323} = 10.11$, $p < 0.001$), interaction ($F_{33,323} = 0.75$, $p =$ NS). Bonferroni post hoc comparison—trial no. 9: naïve versus stressed $*p < 0.05$, versus shCON-infected and stressed $*p < 0.05$, versus shAChE-infected and stressed $p =$ NS. **e** Representative illustrations of mice swimming tracks in the MWM probe test (*gray circles*: place of the missing platform in quadrant #1): *Bottom* shAChE stressed mouse. *Top* shCON stressed mouse. **f** Naïve and shAChE stressed groups display more crosses over the previously situated-platform quadrant. Two-way ANOVA: quadrant ($F_{3,100} = 9.95$, $p < 0.0001$), treatment ($F_{3,100} = 0.002$, $p =$ NS), interaction ($F_{9,100} = 3.38$, $p < 0.012$). Bonferroni post hoc comparison for quadrant #1 (where the platform was previously situated): Naïve versus stressed $*p < 0.05$, versus shCON-infected and stressed $*p < 0.05$, versus shAChE-infected and stressed $p =$ NS; shCON-infected and stressed versus shAChE-infected and stressed $*p < 0.05$

(Pearson's test: $r = -0.58$; $p < 0.01$; Fig. 5a). Normal AChE mRNA levels were already retrieved at this time following footshock stress; however, stressed and control

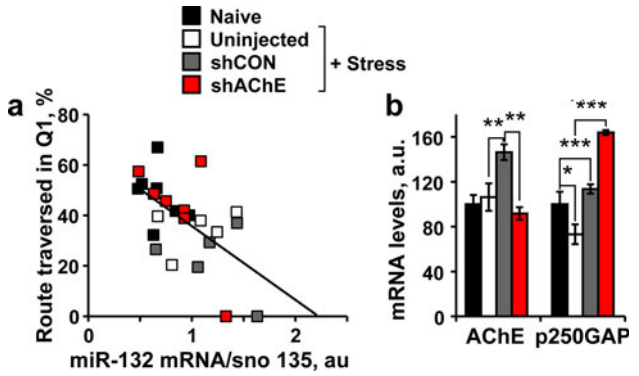

Fig. 5 Hippocampal miR-132 levels show inverse association with the post-stress cognitive performance. **a** Significant negative correlation between hippocampal miR-132 levels and the route traversed in the missing platform quadrant (Q1) in the probe test (Pearson's test: $r = -0.58$; $p < 0.01$). **b** Suppressed hippocampal AChE-S (One-way ANOVA: $F_{3,24} = 7.36$, $p < 0.001$; Post hoc: naïve versus shCON $**p < 0.001$; shCON versus shAChE $**p < 0.01$) and inverse elevation in p250GAP (One-way ANOVA: $F_{3,25} = 24.94$, $p < 0.001$; Post hoc: naïve versus stress $*p < 0.05$, versus shAChE $***p < 0.0001$; stress versus shAChE $***p < 0.0001$) mRNA levels in naïve, stressed, shCON stressed versus shAChE stressed mice. Note that neither AChE mRNA nor p250GAP mRNA levels showed association with the transverse route, attributing the cognitive decline to miR-132 itself

virus-injected mice but not stressed and shRNA injected mice showed AChE mRNA up-regulation (one-way ANOVA: $p < 0.001$, Fig. 5b). Furthermore, as observed in the predator scent test, p250GAP was down-regulated following footshock stress, and intercepting AChE and miR-132 up-regulation resulted in enlarged p250GAP increases (one-way ANOVA: $p < 0.001$; Fig. 5b). However, neither AChE-S mRNA nor p250GAP levels were associated to the cognitive performance.

Chronic hippocampal miR-132 increases associate with AChE-S and p250GAP decreases

To further challenge the causal association between miR-132 and stress-inducible cognitive malfunctioning, we sought an experimental model where miR-132 would be elevated and AChE-S would be diminished. The AChE-R over-expressing TgR mice present such a system. In TgR mice, enforced expression of the human hAChE-R transcript leads to excessive ACh hydrolysis which in turn elevates brain miR-132 levels (Shaked et al. 2009). The elevated miR-132 may target nascent host AChE-S mRNA but not the transgenic 3′UTR-null AChE-R transcripts (Fig. 6a). Correspondingly, TgR mice show an anxiogenic-like phenotype accompanied by hyper-reactivity to nicotine (Salas et al. 2008). Hippocampal miR-132 levels increased by ~2.7-fold in TgR mice compared to non-transgenic FVB/Ns (Student's t test: $p < 0.001$; Fig. 6b). This predictably led to suppression of both host AChE-S and yet

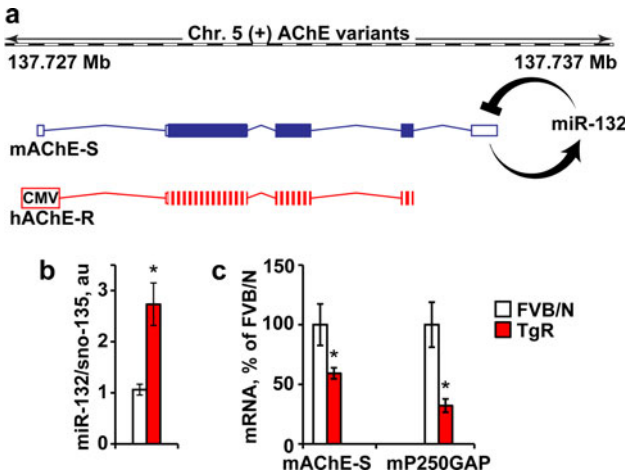

Fig. 6 Hippocampal miR-132 elevation and suppressed AChE-S and p250GAP in TgR mice. **a** The mouse AChE gene in chromosome 5 encodes the miR-132-targeted synaptic mAChE-S transcript, whereas the CMV-regulated transgenic 3′ UTR-null human AChE-R is miR-132 refractory. **b** Hippocampal miR-132 mRNA levels are increased by 2.7-fold in TgR compared to non-transgenic FVB/N mice (Student's t test, $t_{19} = 3.72$, $^*p < 0.001$). **c** Hippocampal AChE-S and p250GAP mRNA levels, are both reduced in TgR versus FVB/N mice (Student's t tests: $^*p < 0.05$)

more so, of p250GAP levels (Student's t test: $p < 0.05$; Fig. 6c). Therefore, if AChE-S suppression could by itself prevent stress-inducible cognitive decline, TgR mice should show no such decline; but if miR-132 increases are the cause, then these mice should present a stress phenotype.

Chronic AChE-S suppression associates with intensified cholinergic hyper-excitation

The AChE-R transgene avoids miR-132 surveillance owing to the lack of its native 3′-UTR (Fig. 7a). Therefore, the TgR brain presents continuous excess of AChE-R which cannot be suppressed, mimicking prolonged conditions of stress (Meshorer and Soreq 2006). Of note, choline acetyl transferase (ChAT)-expressing cholinergic neurons appeared in the engineered brains in normal numbers and size, with a normal symmetric distribution between right and left hemispheres. In general, the engineered AChE-R protein accumulated in cholinoceptive brain regions that tend to express the primary synaptic AChE-S variant [e.g., the CA1 and dentate gyrus (DG) in the hippocampus and the entorhinal cortex]. Typically, the neuronal cytoplasm, nucleus and dendrite(s), but not axons, were stained (Fig. 7b–e). Furthermore, TgR mice presented an extreme sensitivity to cholinergic stimulators. Thus, intraperitoneal exposure to 25 mg/kg of the muscarinic agonist pilocarpine (Dickson and Alonso, 1997) induced massive up-regulation of AChE-R in multiple cholinergic brain regions (Fig. 7f, g). Specifically, the hippocampus and entorhinal cortex showed

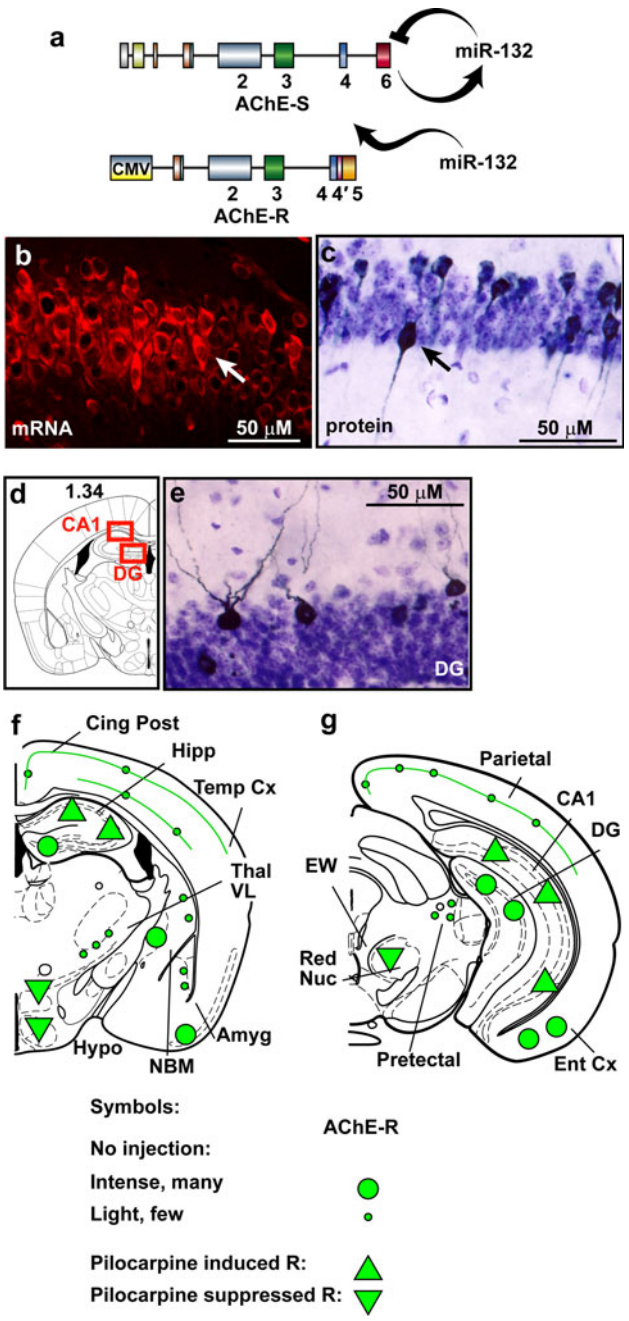

Fig. 7 miR-132-refractory AChE excess induces cholinergic hyper-reactivity. **a** Mouse AChE-S, but not transgenic AChE-R with a truncated 3′-UTR, is recognized by miR-132. **b** CA1 TgR neurons display higher than background expression of human AChE-R mRNA. **c–d** CA1 and dentate gyrus (DG) TgR neurons express higher than background human AChE-R protein. **f–g** Schemes of TgR coronal brain sections showing mouse and transgenic-human AChE-R labeling patterns in hippocampal regions (e.g., dentate gyrus, DG, CA1), subcortical regions [e.g. red nucleus (RN), lateral hypothalamus (LH), amygdala (Amyg)] and in the entrohinal cortex (Ent Cx). *Large* and *small green circles* denote intense or faint transgenic protein expression, respectively. *Green triangles* show intracellular increases (*up*) or decreases (*down*) in host and transgenic protein expression under pilocarpine treatment, respectively

numerous AChE-expressing cells with further intensified labeling under pilocarpine treatment. Under control conditions, several regions showed intense AChE-R labeling; but, pilocarpine treatment caused massive AChE-R elevation throughout the hippocampus (Fig. 7f). Yet more specifically, both TgR and strain-matched FVB/N control mice showed intensified labeling under pilocarpine administration compared to saline-injected mice of the Ca^{2+}-responsive CREB-dependent c-fos mRNA, associated with contextual fear conditioning (two-way ANOVA: $p < 0.05$; Fig. 8a). The c-fos labeling pattern largely overlapped the observed AChE protein increases in the hippocampal CA1 region of the transgenic mice, revealing an hyper-excitatory sensitivity (Frankland et al. 2004) with c-fos significantly correlated to AChE-R labeling (Pearson's test: saline $r = 0.86$, $p < 0.05$; pilocarpine $r = 0.77$, $p < 0.05$; Fig. 8b, c).

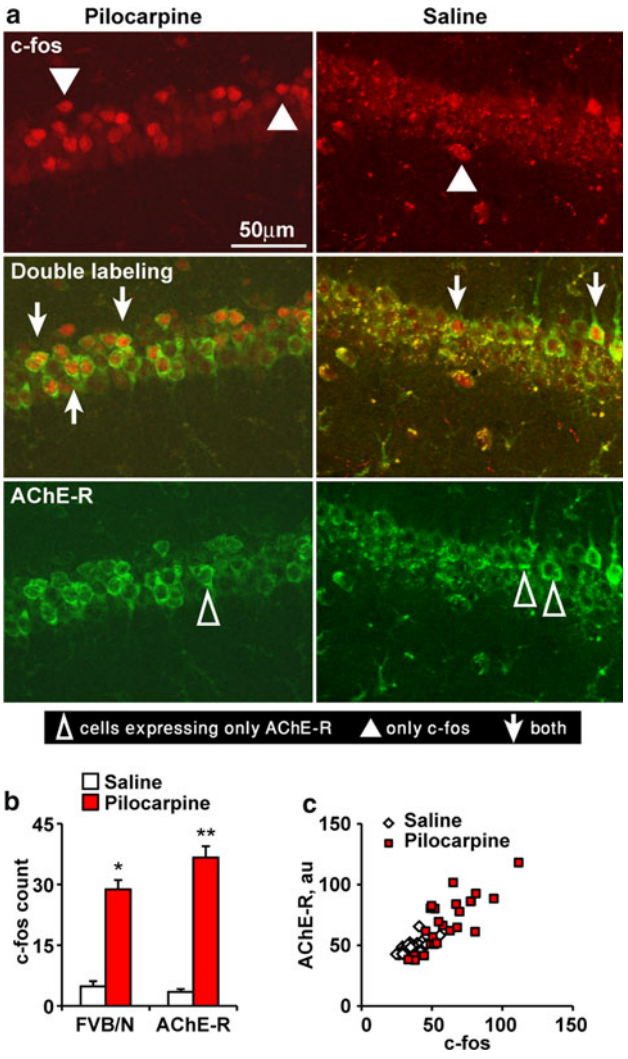

Fig. 8 Pilocarpine induces robust hyperactivation of transgene and c-fos expression in the TgR brain. **a** Pilocarpine induces CA1 c-fos and AChE-R protein increases in TgR mice. **b** Pilocarpine-induced c-fos activation in the CA1 TgR hippocampus: two-way ANOVA shows a significant effect of treatment ($F_{1,19} = 226$, $p < 0.0001$) with a significant interaction between strain and treatment ($F_{2,19} = 5.88$, $p < 0.05$). **c** AChE-R labeling associates with c-fos activation. Pearson's test: for saline $r = 0.86$, $p < 0.05$ and for pilocarpine $r = 0.77$, $p < 0.05$

TgR mice show motion and cognitive malfunctioning

Nocturnal activity monitoring of TgR mice versus non-transgenic controls revealed interchangeable hyper- and hypo-locomotion activity of the transgenics during the dark, but not the light phase of the day compared to controls (Fig. 9a, ANOVA repeated measures: $p < 0.001$). Given parallel, yet distinct changes in the nocturnal activity of mice over-expressing the synaptic AChE-S variant (Cohen et al. 2002), the altered nocturnal activity of the TgR mice likely reflects changes in cholinergic signaling. At the molecular level, hippocampal host AChE-S protein amounts were 55% reduced in TgR mice compared to FVB/N controls (t test: $p < 0.01$; Fig. 9b). To evaluate learning capacities and adaptive behavior, we subjected

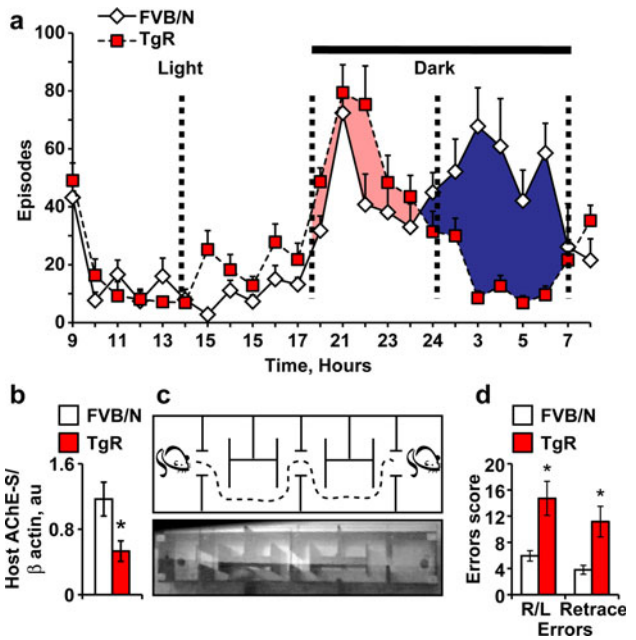

Fig. 9 TgR mice show nocturnal hyper locomotion, suppressed ACHE-S and impaired memory. **a** Nocturnal locomotion patterns of TgR versus FVB/N mice. One-way ANOVA: *Light* $F_{1,22} = 0.4$, $p =$ NS; *Dark* $F_{1,22} = 79.02$, $p < 0.001$. **b** Reduced hippocampal mAChE-S protein levels in TgR mice compared to FVB/N mice (Student's t test: $t_{13} = 2.71$, $^*p < 0.01$). **c** A serial maze task requires a water-deprived mouse to find a sweetened water reward at each end of the maze. The mouse must shuffle five times between the two ends of the maze to obtain five rewards. **d** TgR mice display lower serial maze performance than FVB/Ns. Right/left errors: $F_{1,33} = 9.97$; Retrace errors: $F_{1,33} = 9.37$, $^*p < 0.005$. ANOVA with repeated measures reveals a significant transgene effect in the two measures of performance

these mice to the serial choice maze and measured the animals' ability to avoid right or left turning and/or retrace errors (See Fig. 9c for a scheme of the maze). The cognitive test was conducted during the light phase of the day where no changes in total locomotion activity were observed between the two tested groups. TgR mice displayed significantly more right/left choice errors and retrace errors compared to control FVB/N mice (two-way ANOVA: $p < 0.005$; Fig. 9d). Close examination of videotaped maze behavior revealed two major types of error: "trapping behavior"—running in a repeated path several times without correction, and lack of spatial orientation with respect to reward location, manifested in repeated visits at the end of the maze where the last reward was given and hence no reward was to be expected. Our tests of sensory-motor function did not reveal deficits (Online Resources: Methods) and thus excluded the possibility that trapping behavior was due to the secondary effects of the transgenic intervention.

Stress-inducible total alterations and inter-individual variability in miR-132 and p250GAP

Our working hypothesis predicted that the key processes which are activated under stress conditions would be common to different animal strains and stress paradigms. Therefore, we compared the outcome of the three models we studied integrated together by calculating the percentage change under stress in specific hippocampal transcripts. This analysis again showed increases in miR-132 in both the predator scent (*t* test: $p < 0.01$) and the AChE-R excess models ($p < 0.01$), but not in the footshock stress under shAChE, which led to miR-132 decreases ($p < 0.05$); an accompanying decline in p250GAP in both models ($p < 0.01$ and $p < 0.05$ for the predator scent and AChE-R excess models, respectively) with miR-132 increases. In addition, in all three models, the stress-inducible changes in the hippocampal levels of miR-132 and its p250GAP and AChE targets showed inverse patterns of individual variability. Thus, both predator-stressed C57BI/6J and the chronically anxious TgR FVB/N mice showed larger inter-animal hippocampal miR-132 variability compared to matched controls. Inversely, they both presented smaller p250GAP variability under stress than in control mice (Fig. 10, Online Resources Fig. 4), suggesting that miR-132 changes serve to mitigate p250GAP variability under stress in these two models. In comparison, C57BI/6J mice subjected to shAChE knockdown predictably showed a tendency to reduce AChE levels (60–80% of control levels; $p < 0.05$), while p250GAP levels were elevated in this model ($p < 0.5$; Fig. 10). These findings are compatible with the hypothesis that the inter-individual variability in hippocampal miR-132 is inversely interlocked with that of

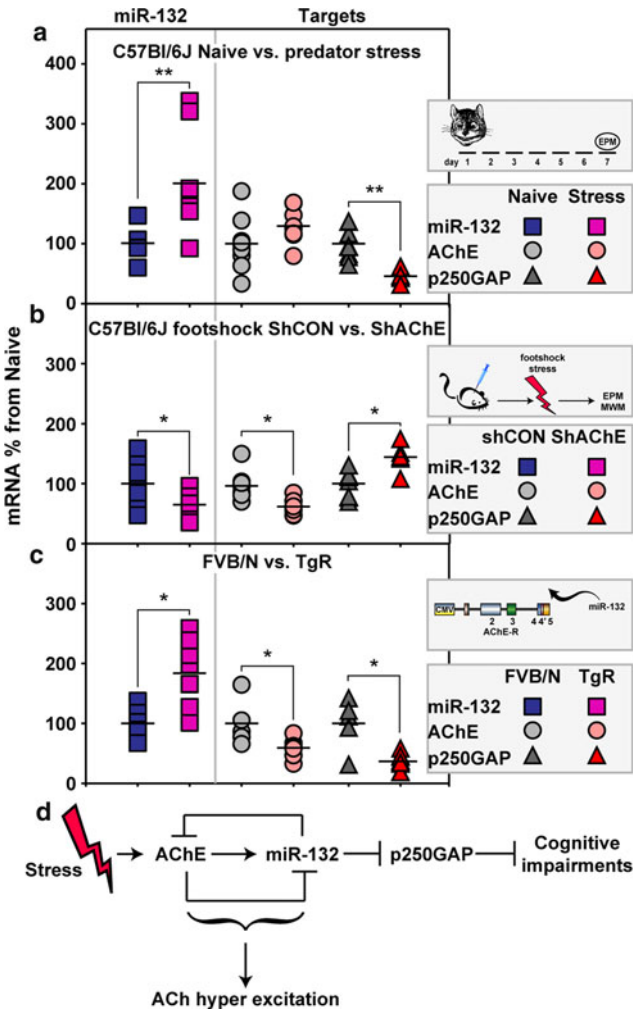

Fig. 10 Integrated analysis of the 3 stress models. Shown in fold changes from controls are the inter-animal variability values and mean changes in hippocampal miR-132, AChE and p250GAP transcript levels in the predator scent (**a**, Student's *t* test: miR-132 $^{**}p < 0.01$, AChE p = NS, p250GAP $^{**}p < 0.01$), footshock (**b**, Student's *t* test: miR-132 $^{*}p < 0.05$, AChE $^{*}p < 0.05$, p250GAP $^{*}p < 0.05$) and transgenic AChE (**c**, Student's *t* test: miR-132 $^{**}p < 0.01$, AChE $^{*}p < 0.05$, p250GAP $^{*}p < 0.05$) stress models employed in our study. **d** Scheme of the proposed mechanism involved

p250GAP. Our analysis thus attributes the observed stress-inducible cholinergic hyper-excitation to the feed-forward regulation of miR-132 and AChE transcripts, and shows that avoiding p250GAP reduction and the corresponding breadth of inter-individual variability in miR-132 associates with stress-inducible cholinergic hyper excitation and cognitive impairments (Fig. 10d).

Discussion

Using three different mouse stress models, we found long-lasting stress-inducible enhancement of both the levels and the individual variability in hippocampal miR-132

expression. This phenomenon was accompanied by the suppression of the levels of hippocampal AChE and the GTPase activator p250GAP, which are both validated miR-132 targets. Knockdown of AChE production greatly limited miR-132 increases in a footshock stress model, suggesting continuous surveillance by cholinergic signaling of miR-132 levels in the hippocampal which is disrupted under psychological stress due to AChE over-production. Suppressing AChE further prevented footshock stress-inducible damages in cognition, but not anxiety, attributing to miR-132 a regulatory role over post-stress cognition but not anxiety. Corroborating this finding, engineered mice with chronic excess of both miR-132 and engineered AChE showed an anxiogenic-like phenotype, impaired locomotion and cognition, and cholinergic hyper-excitation when exposed to pilocarpine. Of note, hippocampal AChE mRNA levels remained elevated 7 days following predator scent test and 14 days following footshock stress accompanied by chronic hippocampal lentiviral infection. In the pre-frontal cortex, we found weeks-long elevation of AChE following mild stress (Meshorer et al. 2005). In the hippocampus, we noted such elevation during 1 h and 1 day post-stress (Kaufer et al. 1998, Nijholt et al. 2004). AChE levels were normal in mice 14 days following footshock stress alone thus indicates the transient nature of this stress in the hippocampus.

In predator-stressed C57BI/6J mice and in FVB/N mice with engineered over-expression of AChE, we found elevated inter-animal variability of hippocampal miR-132 levels which was accompanied by narrower variability of its p250GAP target, suggesting causal links between miR-132 and this neuronal protein. Given the in-bred features of these mouse strains, we hypothesized that the stress-inducible inter-animal variability in hippocampal miR-132 reflects life-long differences in individual experience which mediate these changes. Reinforcing this notion, personal experience determines much of the stress reactions in human patients with post-traumatic stress disorder (Feder et al. 2009).

Both miR-132 and AChE transcription are controlled by CREB (Shaked et al. 2009), which is notably involved in learning and memory, neural growth and by the neuronal growth factor BDNF associated with cholinergic functioning (Cogswell et al. 2008; Im et al. 2010; Wayman et al. 2008). Correspondingly, individual differences in response to chronic stress were recently attributed to hippocampal BDNF (Taliaz et al. 2011). Also, contextual fear conditioning increases pri-miR-132 levels in the mouse hippocampus (Ponomarev et al. 2010) and in the hippocampus of chronically-stressed rats (Meerson et al. 2010), and the cholinergic agonist pilocarpine leads to a transient up-regulation of pri- and mature-miR-132 (Nudelman et al. 2010). The observed pilocarpine and nicotine-inducible (Salas et al. 2008) hyper-excitation in TgR mice is likely due to the failure of miR-132 in these mice to suppress AChE. This hypothesis is reinforced by the co-expression of TgR AChE with the early immediate protein c-fos, which is expressed in neurons whose activity is strongly stimulated by synaptic input (Dragunow and Faull 1989; Frankland et al. 2004). c-fos is also essential for hippocampus-dependent learning and memory (Fleischmann et al. 2003) and represents part of the signal transduction cascade underlying the molecular basis of long-term potentiation (Miyamoto 2006), suggesting relevance for the observed cognitive impairments in TgR mice. In stressed wild type mice, however, activation of the AChE glucocorticoid-responsive element also takes place (Meshorer and Soreq 2006). This might reduce ACh levels and consequently suppress CREB-inducible miR-132 transcription, regaining homeostasis. Hippocampal miR-132 was not up-regulated following stress when AChE-S was suppressed is compatible with proposed inter-locked regulation of these two stress-inducible genes (Fig. 10d).

Cre-lox mediated deletion of miR-132 in newborn hippocampal neurons decreases dendrite length and arborization in adult mice (Magill et al. 2010), supporting a long-lasting role for miR-132 in neuronal differentiation, synaptogenesis and maintenance. The GTPase activator p250GAP emerges as an additional target of miR-132 which is involved in mediating the stress-inducible cognitive malfunctioning. Suppressing p250GAP in cultured cortical neurons enhances neurite sprouting, similar to the neurological reaction following stress (Kawashima et al. 2010). Both neuronal activity and the $GABA_A$ inhibitor bicuculline induce miR-132 transcription, which further down-regulates p250GAP and might enhance neurite growth (Wayman et al. 2008). Also, miR-132 is up-regulated during post-natal development, when massive neurite sprouting occurs; miR-132-targeted antisense oligonucleotides attenuate neurite growth (Ponomarev et al. 2010). The reported link between p250GAP and the NMDA receptor (Nakazawa et al. 2003) further supports a causal role in the post-stress cognitive impairments for p250GAP suppression. Likewise, engineered anti-sense suppression of AChE modulates neuronal sprouting in the mouse hippocampus (Sklan et al. 2006). Our findings of miR-132 excess in the hippocampus of mature TgR mice and in footshock-stressed mice over a month after the insult, and 7 days post-predator scent stress are compatible with the hypothesis that the long-term dual suppression of AChE and p250GAP in the hippocampus might serve as a compensatory mechanism to balance the damages associated with excessive neuronal sprouting.

AChE suppression prevents both miR-132 increases and the accompanying cognitive malfunctioning that suggests the stress-associated changes in neurite sprouting is a

pivotal cause of these damages, and opens new venues for treating trauma patients by mitigating irreversible changes in their neuronal network. Nevertheless, our study did not exclude the involvement of other experimentally validated miR-132 targets. For example, the miR-132-targeted light-induced transcription regulatory factor X 4 (RFX4), abundant in the supra-chiasmatic nucleus (SCN) of the hypothalamus, regulates biological clocks and rhythms (Alvarez-Saavedra et al. 2011; Cheng and Obrietan 2007). In wild type mice, miR-132 levels are lower during the dark part of the circadian cycle in the SCN (Cheng et al. 2007). The nocturnal locomotive fluctuations in the TgR mice may therefore reflect circadian variations in ACh levels, (Erb et al. 2001) which lead to uncontrolled miR-132 and RFX4 levels. The miR-132/-212 cluster also targets the Rett syndrome-related MeCP2 co-factor of the neuronal transcription silencer REST (Klein et al. 2007). REST binding to the regulatory huntingtin protein is impaired during the progression of Huntington's disease (Packer et al. 2008), suggesting parallel stress-associated effects. Inversely, rapid ischemic pre-conditioning, which protects the brain from subsequent prolonged ischemia (Lusardi et al. 2010) is accompanied by miR-132 decreases and MeCP2 increases. MiR-132 also targets the fragile-X mental retardation protein FMRP, knockdown of which abolishes the morphological effects of miR-132 transfection. This suggests competitive interaction between FMRP and p250GAP which may balance out the miR-132-mediated effect on neuronal sprouting (Wayman et al. 2008). In addition, miR-132 is predicted to target several ion channels, and might thus affect cell excitability; correspondingly, over-expressed pre-miR-132 potentiates glutamate, NMDA, or K^+-mediated depolarization of cultured neurons, suggesting global involvement in regulating neurotransmission and plasticity (Wibrand et al. 2010; Edbauer et al. 2010) which may either be direct or function through p250GAP. The multitude targets of neuronal-expressed miRs thus point at combinatorial, rather than single miR-target relevance.

Acknowledgments The authors are grateful to Drs. O. Cohen and G. Zimmerman (Jerusalem) for their contribution to this study. Also acknowledged is support by the Israel Science Foundation Legacy Heritage Biomedical Science Partnership (Grant No. 378/11), the Gatsby Foundation and the German Research Foundation Trilateral Cooperation Program (to H.S.). G.S. was the incumbent of an Eshkol post-doctoral fellowship by the Israel Ministry of Science, M.H. and S.B. were both awarded pre-doctoral fellowships by the Edmond and Lily Safra Center for Brain Sciences.

Conflict of interest The authors declare that they have no conflict of interest.

References

Alvarez-Saavedra M, Antoun G, Yanagiya A, Oliva-Hernandez R, Cornejo-Palma D, Perez-Iratxeta C, Sonenberg N, Cheng HY (2011) miRNA-132 orchestrates chromatin remodeling and translational control of the circadian clock. Hum Mol Genet 20(4):731–751. doi:10.1093/hmg/ddq519

Bartel DP (2009) MicroRNAs: target recognition and regulatory functions. Cell 136(2):215–233. doi:10.1016/j.cell.2009.01.002

Berson A, Knobloch M, Hanan M, Diamant S, Sharoni M, Schuppli D, Geyer BC, Ravid R, Mor TS, Nitsch RM, Soreq H (2008) Changes in readthrough acetylcholinesterase expression modulate amyloid-beta pathology. Brain 131(Pt 1):109–119

Blank T, Nijholt I, Eckart K, Spiess J (2002) Priming of long-term potentiation in mouse hippocampus by corticotropin-releasing factor and acute stress: implications for hippocampus-dependent learning. J Neurosci 22(9):3788–3794

Carter CS, Braver TS, Barch DM, Botvinick MM, Noll D, Cohen JD (1998) Anterior cingulate cortex, error detection, and the online monitoring of performance. Science 280(5364):747–749

Chen CZ, Li L, Lodish HF, Bartel DP (2004) MicroRNAs modulate hematopoietic lineage differentiation. Science 303(5654):83–86

Cheng HY, Obrietan K (2007) Revealing a role of microRNAs in the regulation of the biological clock. Cell Cycle 6(24):3034–3035 pii: 5106

Cheng HY, Papp JW, Varlamova O, Dziema H, Russell B, Curfman JP, Nakazawa T, Shimizu K, Okamura H, Impey S, Obrietan K (2007) MicroRNA modulation of circadian-clock period and entrainment. Neuron 54(5):813–829

Cogswell JP, Ward J, Taylor IA, Waters M, Shi Y, Cannon B, Kelnar K, Kemppainen J, Brown D, Chen C, Prinjha RK, Richardson JC, Saunders AM, Roses AD, Richards CA (2008) Identification of miRNA changes in Alzheimer's disease brain and CSF yields putative biomarkers and insights into disease pathways. J Alzheimers Dis 14(1):27–41

Cohen O, Erb C, Ginzberg D, Pollak Y, Seidman S, Shoham S, Yirmiya R, Soreq H (2002) Neuronal overexpression of 'read-through' acetylcholinesterase is associated with antisense-suppressible behavioral impairments. Mol Psychiatry 7(8):874–885

Cohen H, Kaplan Z, Matar MA, Loewenthal U, Kozlovsky N, Zohar J (2006) Anisomycin, a protein synthesis inhibitor, disrupts traumatic memory consolidation and attenuates posttraumatic stress response in rats. Biol Psychiatry 60(7):767–776

Diamond DM, Park CR, Heman KL, Rose GM (1999) Exposing rats to a predator impairs spatial working memory in the radial arm water maze. Hippocampus 9(5):542–552

Dickson CT, Alonso A (1997) Muscarinic induction of synchronous population activity in the entorhinal cortex. J Neurosci 17: 6729–6744

Dragunow M, Faull R (1989) The use of c-fos as a metabolic marker in neuronal pathway tracing. J Neurosci Methods 29(3):261–265

Edbauer D, Neilson JR, Foster KA, Wang CF, Seeburg DP, Batterton MN, Tada T, Dolan BM, Sharp PA, Sheng M (2010) Regulation of synaptic structure and function by FMRP-associated microRNAs miR-125b and miR-132. Neuron 65(3):373–384. doi: 10.1016/j.neuron.2010.01.005

Ellman GL, Courtney KD, Andres V Jr, Feather-Stone RM (1961) A new and rapid colorimetric determination of acetylcholinesterase activity. Biochem Pharmacol 7:88–95

Erb C, Troost J, Kopf S, Schmitt U, Loffelholz K, Soreq H, Klein J (2001) Compensatory mechanisms enhance hippocampal acetylcholine release in transgenic mice expressing human acetylcholinesterase. J Neurochem 77(2):638–646

Farchi N, Ofek K, Podoly E, Dong H, Xiang YY, Diamant S, Livnah O, Li J, Hochner B, Lu WY, Soreq H (2007) Peripheral site

acetylcholinesterase blockade induces RACK1-associated neuronal remodeling. Neurodegener Dis 4(2–3):171–184
Feder A, Nestler EJ, Charney DS (2009) Psychobiology and molecular genetics of resilience. Nat Rev Neurosci 10(6):446–457. doi:10.1038/nrn2649
Filipowicz W, Bhattacharyya SN, Sonenberg N (2008) Mechanisms of post-transcriptional regulation by microRNAs: are the answers in sight? Nat Rev Genet 9(2):102–114
Fleischmann A, Hvalby O, Jensen V, Strekalova T, Zacher C, Layer LE, Kvello A, Reschke M, Spanagel R, Sprengel R, Wagner EF, Gass P (2003) Impaired long-term memory and NR2A-type NMDA receptor-dependent synaptic plasticity in mice lacking c-fos in the CNS. J Neurosci 23(27):9116–9122
Frankland PW, Bontempi B, Talton LE, Kaczmarek L, Silva AJ (2004) The involvement of the anterior cingulate cortex in remote contextual fear memory. Science 304(5672):881–883. doi:10.1126/science.1094804
Goel N, Bale TL (2010) Sex differences in the serotonergic influence on the hypothalamic-pituitary-adrenal stress axis. Endocrinology 151(4):1784–1794
Gray R, Rajan AS, Radcliffe KA, Yakehiro M, Dani JA (1996) Hippocampal synaptic transmission enhanced by low concentrations of nicotine. Nature 383(6602):713–716. doi:10.1038/383713a0
Im H-I, Hollander JA, Bali P, Kenny PJ (2010) MeCP2 controls BDNF expression and cocaine intake through homeostatic interactions with microRNA-212. Nat Neurosci 13(9):1120-–127. http://www.nature.com/neuro/journal/v13/n9/abs/nn.2615.html#supplementary-information
Karnovsky MJ, Roots L (1964) A "Direct-Coloring" thiocholine method for cholinesterases. J Histochem Cytochem 12:219–221
Kaufer D, Friedman A, Seidman S, Soreq H (1998) Acute stress facilitates long-lasting changes in cholinergic gene expression. Nature 393(6683):373–377
Kawashima H, Numakawa T, Kumamaru E, Adachi N, Mizuno H, Ninomiya M, Kunugi H, Hashido K (2010) Glucocorticoid attenuates brain-derived neurotrophic factor-dependent upregulation of glutamate receptors via the suppression of microRNA-132 expression. Neuroscience 165(4):1301–1311. doi:10.1016/j.neuroscience.2009.11.057
Klein ME, Lioy DT, Ma L, Impey S, Mandel G, Goodman RH (2007) Homeostatic regulation of MeCP2 expression by a CREB-induced microRNA. Nat Neurosci 10(12):1513–1514
Krol J, Loedige I, Filipowicz W (2010) The widespread regulation of microRNA biogenesis, function and decay. Nat Rev Genet 11(9):597–610. doi:10.1038/nrg2843
Lusardi TA, Farr CD, Faulkner CL, Pignataro G, Yang T, Lan J, Simon RP, Saugstad JA (2010) Ischemic preconditioning regulates expression of microRNAs and a predicted target, MeCP2, in mouse cortex. J Cereb Blood Flow Metab 30(4):744–756. doi:10.1038/jcbfm.2009.253
Magill ST, Cambronne XA, Luikart BW, Lioy DT, Leighton BH, Westbrook GL, Mandel G, Goodman RH (2010) MicroRNA-132 regulates dendritic growth and arborization of newborn neurons in the adult hippocampus. Proc Natl Acad Sci USA 107(47):20382–20387. doi:10.1073/pnas.1015691107
McEwen BS, Gianaros PJ (2011) Stress- and allostasis-induced brain plasticity. Annu Rev Med 62:431–445. doi:10.1146/annurev-med-052209-100430
Meerson A, Cacheaux L, Goosens KA, Sapolsky RM, Soreq H, Kaufer D (2010) Changes in brain microRNAs contribute to cholinergic stress reactions. J Mol Neurosci 40(1–2):47–55
Meshorer E, Bryk B, Toiber D, Cohen J, Podoly E, Dori A, Soreq H (2005) SC35 promotes sustainable stress-induced alternative splicing of neuronal acetylcholinesterase mRNA. Mol Psychiatry 10(11):985–997
Meshorer E, Soreq H (2002) Pre-mRNA splicing modulations in senescence. Aging Cell 1(1):10–16
Meshorer E, Soreq H (2006) Virtues and woes of AChE alternative splicing in stress-related neuropathologies. Trends Neurosci 29(4):216–224
Meshorer E, Erb C, Gazit R, Pavlovsky L, Kaufer D, Friedman A, Glick D, Ben-Arie N, Soreq H (2002) Alternative splicing and neuritic mRNA translocation under long-term neuronal hypersensitivity. Science 295(5554):508–512
Miyamoto E (2006) Molecular mechanism of neuronal plasticity: induction and maintenance of long-term potentiation in the hippocampus. J Pharmacol Sci 100(5):433–442
Nakazawa T, Watabe AM, Tezuka T, Yoshida Y, Yokoyama K, Umemori H, Inoue A, Okabe S, Manabe T, Yamamoto T (2003) p250GAP, a novel brain-enriched GTPase-activating protein for Rho family GTPases, is involved in the N-methyl-d-aspartate receptor signaling. Mol Biol Cell 14(7):2921–2934. doi:10.1091/mbc.E02-09-0623
Nijholt I, Farchi N, Kye M, Sklan EH, Shoham S, Verbeure B, Owen D, Hochner B, Spiess J, Soreq H, Blank T (2004) Stress-induced alternative splicing of acetylcholinesterase results in enhanced fear memory and long-term potentiation. Mol Psychiatry 9(2):174–183
Nudelman AS, DiRocco DP, Lambert TJ, Garelick MG, Le J, Nathanson NM, Storm DR (2010) Neuronal activity rapidly induces transcription of the CREB-regulated microRNA-132, in vivo. Hippocampus 20(4):492–498. doi:10.1002/hipo.20646
Packer AN, Xing Y, Harper SQ, Jones L, Davidson BL (2008) The bifunctional microRNA miR-9/miR-9* regulates REST and CoREST and is downregulated in Huntington's disease. The Journal of neuroscience : the official journal of the Society for Neuroscience 28(53):14341–14346. doi:10.1523/JNEUROSCI.2390-08.2008
Ponomarev ED, Veremeyko T, Barteneva N, Krichevsky AM, Weiner HL (2010) MicroRNA-124 promotes microglia quiescence and suppresses EAE by deactivating macrophages via the C/EBP-[alpha]-PU.1 pathway. Nat Med advance online publication. http://www.nature.com/nm/journal/vaop/ncurrent/abs/nm.2266.html#supplementary-information
Quartermain D, Mower J, Rafferty MF, Herting RL, Lanthorn TH (1994) Acute but not chronic activation of the NMDA-coupled glycine receptor with D-cycloserine facilitates learning and retention. Eur J Pharmacol 257(1–2):7–12
Rana TM (2007) Illuminating the silence: understanding the structure and function of small RNAs. Natl Rev Mol Cell Biol 8(1):23–36
Salas R, Main A, Gangitano DA, Zimmerman G, Ben-Ari S, Soreq H, De Biasi M (2008) Nicotine relieves anxiogenic-like behavior in mice that overexpress the read-through variant of acetylcholinesterase but not in wild-type mice. Mol Pharmacol 74(6):1641–1648
Shaked I, Meerson A, Wolf Y, Avni R, Greenberg D, Gilboa-Geffen A, Soreq H (2009) MicroRNA-132 potentiates cholinergic anti-inflammatory signaling by targeting acetylcholinesterase. Immunity 31(6):965–973
Sklan EH, Berson A, Birikh KR, Gutnick A, Shahar O, Shoham S, Soreq H (2006) Acetylcholinesterase Modulates Stress-Induced Motor Responses Through Catalytic and Noncatalytic Properties. Biol Psychiatry 60:741–751
Soreq H, Wolf Y (2011) NeurimmiRs: microRNAs in the neuroimmune interface. Trends Mol Med 17(10):548–555
Sternfeld M, Shoham S, Klein O, Flores-Flores C, Evron T, Idelson GH, Kitsberg D, Patrick JW, Soreq H (2000) Excess "read-through" acetylcholinesterase attenuates but the "synaptic" variant intensifies neurodeterioration correlates. Proc Natl Acad Sci USA 97(15):8647–8652

Taliaz D, Loya A, Gersner R, Haramati S, Chen A, Zangen A (2011) Resilience to chronic stress is mediated by hippocampal brain-derived neurotrophic factor. The Journal of neuroscience : the official journal of the Society for Neuroscience 31(12): 4475–4483. doi:10.1523/JNEUROSCI.5725-10.2011

Vo N, Klein ME, Varlamova O, Keller DM, Yamamoto T, Goodman RH, Impey S (2005) A cAMP-response element binding protein-induced microRNA regulates neuronal morphogenesis. Proc Natl Acad Sci USA 102(45):16426–16431

Wayman GA, Davare M, Ando H, Fortin D, Varlamova O, Cheng HY, Marks D, Obrietan K, Soderling TR, Goodman RH, Impey S (2008) An activity-regulated microRNA controls dendritic plasticity by down-regulating p250GAP. Proc Natl Acad Sci USA 105(26):9093–9098

Wibrand K, Panja D, Tiron A, Ofte ML, Skaftnesmo KO, Lee CS, Pena JT, Tuschl T, Bramham CR (2010) Differential regulation of mature and precursor microRNA expression by NMDA and metabotropic glutamate receptor activation during LTP in the adult dentate gyrus in vivo. Eur J Neurosci 31(4):636–645. doi: 10.1111/j.1460-9568.2010.07112.x